mathematics

MDPI

Article

Minimization of Active Power Loss Using Enhanced Particle Swarm Optimization

Samson Ademola Adegoke [1,*], Yanxia Sun [1,*] and Zenghui Wang [2]

[1] Department of Electrical and Electronic Engineering Science, University of Johannesburg, Johannesburg 2006, South Africa
[2] Department of Electrical Engineering, University of South Africa, Florida 1709, South Africa; wangz@unisa.ac.za
* Correspondence: adsam4u@gmail.com (S.A.A.); ysun@uj.ac.za (Y.S.)

Abstract: Identifying the weak buses in power system networks is crucial for planning and operation since most generators operate close to their operating limits, resulting in generator failures. This work aims to identify the critical/weak node and reduce the system's power loss. The line stability index (L_{mn}) and fast voltage stability index (FVSI) were used to identify the critical node and lines close to instability in the power system networks. Enhanced particle swarm optimization (EPSO) was chosen because of its ability to communicate with better individuals, making it more efficient to obtain a prominent solution. EPSO and other PSO variants minimized the system's actual/real losses. Nodes 8 and 14 were identified as the critical nodes of the IEEE 9 and 14 bus systems, respectively. The power loss of the IEEE 9 bus system was reduced from 9.842 MW to 7.543 MW, and for the IEEE 14 bus system, the loss was reduced from 13.775 MW of the base case to 12.253 MW for EPSO. EPSO gives a better active power loss reduction and improves the node's voltage profile than other PSO variants and algorithms in the literature. This suggests the feasibility and suitability of EPSO to improve the grid voltage quality.

Keywords: voltage stability; identification of weak bus; FVSI and L_{mn}; diminish power loss; PSO variants; EPSO

MSC: 90C11; 90C30

Citation: Adegoke, S.A.; Sun, Y.; Wang, Z. Minimization of Active Power Loss Using Enhanced Particle Swarm Optimization. *Mathematics* **2023**, *11*, 3660. https://doi.org/10.3390/math11173660

Academic Editor: Nicu Bizon

Received: 10 July 2023
Revised: 15 August 2023
Accepted: 17 August 2023
Published: 24 August 2023

1. Introduction

Voltage stability (VS) is a major focus of modern power system (PS) utility companies. Therefore, VS is the ability of systems to keep the voltage profile stable when undergoing large or small disturbances. Different means have been used to improve the voltage profile in modern PS, such as battery storage systems and distributed energy resources (DER) [1–4]. The increase in the infrastructure and load demand rate leads to the high utilization of PS energy equipment. This has made systems experience voltage instability that has led to blackouts in some parts of the world, destruction of some businesses and daily activities, and increased power loss. Based on this problem, this study is motivated by identifying the weak bus that could cause a blackout in a system and reducing system transmission loss, which is caused by a shortage of reactive power (RP), which significantly affects the quality of energy delivery to the consumer end. Environmental and economic factors are two leading causes for establishing a new transmission line (TL). As the load increases, the system is heavily loaded, and maintaining stability becomes difficult; thus, the system operates close to the instability point [5–8]. Evaluation of system stability is based on the node/bus voltage profile. Presently, there are numerous techniques for finding system stability. The line voltage stability index (LVSI) [9], a simplified voltage stability index (SVSI) [10], L-index [11], a global voltage stability index (GVSI) [12], etc. Some classical voltage stability assessments and various techniques have been proposed for weak bus

identification in power system networks. Some of them are genetic algorithms based on support vector machine (GA-VSM) [13], ant colony (AC) [14], electric cactus structure (ECS) [15], and network response structural characteristic (NRSC) [16].

A shortage of RP in a PS network causes a tremendous waste of electricity in the distribution system, resulting in extra emission of carbon and power generation cost. Therefore, reducing losses in transmission line networks (TLN) is essential for system safety. However, the best way to reduce losses in TLs of PS networks is RP optimization (RPO). Two methods used in solving the RPO problem are traditional and evolutionary algorithms. Traditional methods include the Newton–Raphson (NR) method, interior point methods, quadratic programming, and linear programming [17]. Recently, evolution algorithms have been used to solve RPO problems, such as the hybrid pathfinder algorithm (HPFA) [18], hybrid PSO (HPSO-PFA) [17], modified PFA (mPFA) [19], chaotic krill herd [20], ant lion optimizer (ALO) [21], the tree seed algorithm (TSA) [22], and the improved pathfinder algorithm (IPFA) [23]. However, PSO is good in search capacity and has less programming than others [17].

Harish et al. used the fast voltage stability index (FVSI) and line stability index (L_{mn}) to identify the location of flexible alternating current transmission system (FACTS) devices along with PSO, artificial bee colony (ABC), and the hybrid genetic algorithm (H-GA) to find the sizing of the FACTS devices [24]. Also, a novel method for strengthening PS stability was proposed by Jaramillo et al. [25]. FVSI was used to identify the node on which the SVC should be installed under an N-1 scenario. It was reported that the result obtained could reestablish the FVSI in each contingency before the outage [25]. The voltage collapse critical bus index (VCCBI) [26], L-Index, voltage collapse proximity index (VCPI), and modal analysis [27], which are part of voltage stability indices (VSI), were used to identify weak/vulnerable buses in electrical power systems. Power loss reduction was made using a hybrid loop-genetic-based algorithm (HLGBA) [28], the Jaya algorithm (JAYA), diversity-enhanced (DEPSO), etc. [29].

This research considers the identification of critical nodes and loss reduction, which serve as merit over the previous work mentioned above. FVSI and L_{mn} were used to find the critical node in the system based on load flow (LF) results from MATLAB 2018b software (MathWorks, Inc., Natick, MA, USA). FVSI and L_{mn} were chosen because of their efficiency in identifying the weak/vulnerable bus (i.e., the fastness of FVSI and the accuracy of L_{mn}) [30]. The critical node was determined by the value of the indices (i.e., FVSI and L_{mn}). When the indices value reaches unity or is close to unity, that node is the critical node of the system. The reactive powers of all the load buses were increased one after the other to determine the maximum RP on each of the load buses/nodes. Also, each line's value of FVSI and L_{mn} was computed to determine the load-ability limit on each load bus. The ranking was carried out based on the indices value of each node; hence, the node with the highest indices values is the system's critical bus. This bus contained the smallest RP when the load bus was varied. The identified node needs reactive power support to avoid voltage collapse. Also, enhanced PSO (EPSO) was used to minimize the PS network loss along with PSO variants that have been developed by previous research, such as PSO-based time-varying acceleration coefficients (PSO-TVAC) [31], random inertia weight PSO (RPSO), and PSO based on success rate (PSO-SR) [32]. To overcome the premature convergence of PSO, the chosen EPSO was applied, and it uses neighborhood exchange to share more information with the other best individual (neighborhood) to improve itself, which makes it more efficient in getting a prominent solution (i.e., exploitation stage) to optimizing the objective function. The novelty of this research and this paper's contribution is that each particle learns from its own personal and global positions in the PSO algorithm in the social cognitive system. Apart from personal experience and better information received from the search areas, it is advisable to share with better individuals to enhance or improve itself. Therefore, a new acceleration constant (c_3) is added to the original PSO equation, making obtaining the best solution more efficient. Also, additional c_3 gives the swarm the capability to reach the exploitation stage, which helps to overcome the premature convergence of PSO.

However, this paper has contributed by (1) comparing different PSO variants and EPSO for power loss reduction; (2) identifying the power system critical node for the perfect operation of generators to avoid breakdown.

The rest of the paper is structured as follows: Section 2 presents the problem formulation of voltage stability indices and RPO, and Section 3 discusses the PSO, its variants, and EPSO. The results and discussion are presented in Section 4, and the conclusion and future work is the last section.

2. Problem Formulation

2.1. Formulation of Voltage Stability Indices

FVSI and L_{mn} are part of the VSI methods for identifying weak buses. They were formed based on two bus systems. For a system to be stable, the value of FVSI and L_{mn} must be smaller than unity and unstable when it equals unity and above.

2.1.1. FVSI

FVSI was developed [33] based on the concept of a single line of power flow (PF). The FVSI is evaluated by:

$$\text{FVSI} = \frac{4Zj^2Q_1}{V_1^2Xr} \leq 1 \tag{1}$$

where Zj is the impedance, Q_1 is the RP at sending ends, Xr is the reactance of the line, and V_1 is the voltage at the sending end.

2.1.2. L_{mn}

L_{mn} was proposed by the authors of [34]. Using the concept of PF from a single-line diagram, the discriminant of the quadratic voltage equation is set to be higher than or equal to zero. The equation is given below.

$$L_{mn} = \frac{4XQ_2}{[V_1\sin(\theta - \delta)]^2} \leq 1 \tag{2}$$

where θ is the angle of the TL, δ is the power angle, and Q_2 is the RP at receiving end.

2.2. Steps Involve in Identifying Critical Node in EPS

Identifying critical nodes in EPS is essential for delivering stable electricity to the consumer end. The following steps are involved:

1. Input the line and bus data of the IEEE test case;
2. Run the PF solution in MATLAB using the NR method at the base case;
3. Calculate the stability values of FVSI and L_{mn} of the IEEE test system;
4. Gradually increased the RP of the load bus until the values of FVSI and L_{mn} are closer to one (1);
5. The load bus with the highest FVSI and L_{mn} value is selected at the critical node;
6. Steps 1 to 5 are repeated for all the load buses;
7. The highest RP loading is selected and called maximum load-ability;
8. The voltage magnitude at the critical loading of a particular load bus is obtained and is called the critical voltage of a specific load bus.

2.3. Formulation of RPO

The main objective of RPO is to reduce the network's actual power loss.

2.3.1. Objective Function

The main goal of RPO is to reduce the network's actual power losses, which are described as follows.

$$\text{Minimize } f = P_{loss}(x, u) \tag{3}$$

which satisfying

$$\begin{cases} g(x,u) = 0 \\ h(x,u) \leq 0 \end{cases} \tag{4}$$

where $f(x,u)$ is the objective function, $g(x,u)$ is the equality constraints, $h(x,u)$ is the inequality constraints, x is the vector of the state variables, and u is the vector of the control variables.

The real power loss minimization in the TL is given below, and its purpose is to reduce the overall loss in the TLN.

$$Minf = P_{loss} \sum_{K=1}^{N_L} G_k \left(v_i^2 + v_j^2 - 2V_i V_j \cos\theta_{ij} \right) \tag{5}$$

where P_{loss} is the real total losses, k is the branch, G_k is the conductance of the branch k, Vj and V_i is the voltage at the ith and jth bus, N_L is the total number of TL, and θ_{ij} is the voltage angle between bus i and j.

2.3.2. Equality Constraints

The PS network's active and reactive PF equation are called the equality constraints.

$$P_{gi} - P_{di} - V_i \sum_{j=1}^{N} V_j (g_{ij} \cos\theta_{ij} + b_{ij} \sin\theta_{ij}) = 0 \tag{6}$$

$$Q_{gi} - Q_{di} - V_i \sum_{j=1}^{N} V_j (g_{ij} \sin\theta_{ij} - b_{ij} \cos\theta_{ij}) = 0 \tag{7}$$

Here, g_{ij} and b_{ij} are conductance and susceptance, and θ_{ij} is the phase difference of voltages.

2.3.3. Inequality Constraints

Inequality constraints are operational variables that must be kept within acceptable limits.

(1). Generator constraints

$$V_{gi}^{min} \leq V_{gi} \leq V_{gi}^{max} \qquad i = 1 \ldots, N_g \tag{8}$$

$$Q_{gi}^{min} \leq Q_{gi} \leq Q_{gi}^{max} \qquad i = 1 \ldots, N_g \tag{9}$$

(2). Reactive compensation constraints

$$Q_{ci}^{min} \leq Q_{ci} \leq Q_{ci}^{max} \qquad i = 1 \ldots, N_C \tag{10}$$

(3). Transformer tap ratio constraints

$$T_k^{min} \leq T_k \leq T_k^{max} \quad i = 1 \ldots, N_T \tag{11}$$

where V_{gi}^{min} and V_{gi}^{max} are voltage amplitude limits, Q_{gi}^{min} and Q_{gi}^{max} are the generation limits of reactive power, P_{gi}^{min} and P_{gi}^{max} are the limits of active power, Q_{ci}^{min} and Q_{ci}^{max} are the reactive compensation limits, and T_k^{min} and T_k^{max} are the transformer tap limits.

The penalty function is used to make optimization problems more straightforward and rigorous. In other to solve the optimization problem, the penalty function has to be selected. The primary function of the penalty function is to keep system security within the acceptable limits.

$$f_T = f + \lambda_V \sum_{K=1}^{N_B} \left(V_i - V_i^{lim}\right)^2 + \lambda_g \sum_{K=1}^{N_B} \left(Q_{gi} - Q_{gi}^{lim}\right)^2 + \lambda_s \sum_{K=1}^{N_B} \left(S_i - S_i^{lim}\right)^2 \quad (12)$$

where λ_V, λ_g, and λ_s

$$V_i^{lim} = \begin{cases} V_i^{lim}, if\ V_i < V_i^{min} \\ V_i^{lim}, if\ V_i > V_i^{max} \end{cases} \quad (13)$$

$$Q_{gi}^{lim} = \begin{cases} Q_{gi}^{lim}, if\ Q_{gi} < Q_{gi}^{min} \\ Q_{gi}^{lim}, if\ Q_{gi} > Q_{gi}^{max} \end{cases} \quad (14)$$

$$S_i^{lim} = \begin{cases} S_i^{lim}, if\ S_i < S_i^{min} \\ S_i^{lim}, if\ S_i > S_i^{max} \end{cases} \quad (15)$$

3. Particle Swarm Optimization (PSO)

3.1. PSO and Its Variants

3.1.1. Overview of PSO

PSO was created in 1995 by Kennedy and Eberhart [35]. The social behavior of birds and schooling fish was the basis for the population-based stochastic optimization method known as PSO. In the search space, PSO makes use of the promising area. Each particle moves and adjusts its position following its past behavior and the best particle within a decision time. Each particle is identified by a d-dimensional vector that depicts its location in the search space. The position of the vector is represented as a possible solution to the optimization issue. Whenever an iterative process is performed, the velocity is added to update each particle's position [36]. The best particle in the swarm (population) and the distance from the best cognitive both impact the particle's velocity. The formulae for velocity and position are shown below.

$$V_i^{k+1} = wv_i^k + c_1 \times r_1 \left(p_{best} - s_i^k\right) + c_2 \times r_2 \left(g_{best} - s_i^k\right) \quad (16)$$

$$s_i^{k+1} = s_i^k + V_i^{k+1} \quad (17)$$

where V_i^k is the velocity of the particle, s_i^k is the position of the particle, r_1 and r_2 are two randomly generated numbers between (0, 1), c_1 and c_2 are the coefficients of accelerated particles, w is the inertia weight, p_{best} is the personal best, and g_{best} is the global best.

3.1.2. RPSO

In RPSO, the weight factor was usually between 0.5 and 1 [37]. Roy Ghatak et al. claim that the random inertia weight component enhanced the initial objective function. Stocking to the local optimal at the end of the iteration may affect the accuracy of the solution [32]. The value of w is found in Equation (19).

$$w = 0.5 + rand()/2 \quad (18)$$

3.1.3. PSO-SR

To find the best method for the effective management of inertia weight (w), a novel adaptive w was developed based on success rate (SR) [37]. At each iteration, the swarm position is determined using the SR. Indicate that a big value of w is necessary to advance toward the optimal point when the SR is large. Additionally, for a low value, the particle

oscillates around the ideal location and requires a small increase in the w value to reach the perfect result [32].

$$w(t) = \left(w^{max} - w^{min}\right) * \mathrm{SR} + w^{min} \tag{19}$$

where SR is the success rate and is chosen to be 1 (otherwise, it is zero), w^{min} and w^{max} are the minimum and maximum limits of the w [32].

3.1.4. PSO-TVAC

Due to the lack of diversity towards the end of the search area, PSO with PSOTV-w was utilized, which locates the optimal solution more quickly but is less effective at tuning the optimal solution. The accuracy and effectiveness of the PSO to obtain optimal solutions are significantly influenced by the tuning parameter [31,38]. Based on this concept, a TVAC was proposed to enhance the global search at the start of optimization, allowing the particle to move to the global optimum at the end of the search space. As the search progresses, c_1 and c_2 alter over time, decreasing the cognitive components and increasing the social components. This indicates that the particle converges to the global optimum towards the end of the search process due to minor cognitive and greater social components. Additionally, the particle can roam throughout the search area rather than initially gravitating toward the best population due to enhanced cognitive and minor social components [31].

$$C_1 = (C_{1t} - C_{1k})\frac{z}{iter_{max}} + C_{1k} \tag{20}$$

$$C_2 = (C_{2t} - C_{2k})\frac{z}{iter_{max}} + C_{2k} \tag{21}$$

where z is the current iteration, $iter_{max}$ is the maximum iteration, and C_{1k}, C_{1t}, C_{2t}, and C_{2k} are the initial and final values of the cognitive and social acceleration factors. The value for C_{1t} and C_{2k} is 0.5, and 2.5 for C_{1k} and C_{2t} is the most accurate value [39].

3.2. EPSO

To overcome the issue of falling into a local optimal from the standard PSO, the chosen EPSO added some expansion to the basic PSO, such as a constriction factor and a neighborhood model.

3.2.1. Exchange of Neighborhood

Since each particle learns from its own personal and global positions in the PSO algorithm in the social cognitive system, apart from personal experience and better information received from the search areas, it is advisable to share with better individuals to enhance or improve itself [40]. Therefore, using that concept, a new acceleration constant (c_3) is added to the original PSO equation, making it more efficient to obtain the best solution. The additional c_3 gives the swarm the capability to reach the exploitation stage.

$$V_i^{k+1} = \varphi\left(w_1 v_i^k + c_1 r_1 \left(p_{best} - s_i^k\right) + c_2 r_2 \left(g_{best} - s_i^k\right) + c_3 \times r_3 \left(p_{best,\ t} - s_i^k\right)\right) \tag{22}$$

where $p_{best,t}$ is the vector position for an excellent individual domain (i.e., the overall best position), φ is the constriction factor, and r_3 is random numbers in the interval of (0,1).

3.2.2. Implementation of EPSO to RPO

The steps involved in solving the RPO problem are given below, and the flow chart is shown in Figure 1:

1. Initialize: Set the number of particles, initial velocity, the total number of iterations, generator voltages, the transformer tap settings, and accelerated constants;
2. Run load flows to determine the objective function (real power loss) and evaluate the penalty function concerning inequality constraint violation;

3. Counter updating: Update the iter = iter + 1;
4. Evaluate each particle and save the global and personal best positions;
5. Update the velocity as given in Equation (22);
6. Update the position as given in Equation (17);
7. Check whether solutions in Steps 3 and 4 are within the limit; if it is above the limit, apply Equation (12) to keep the violation;
8. The position of the local best should be updated if the current fitness value is smaller than the best one;
9. Update global best;
10. Search for minimum value: The minimum value in all the individual iterations is considered the best solution;
11. Stopping criteria: If the stopping criteria have been satisfied, stop; if not, go back to Step 5.

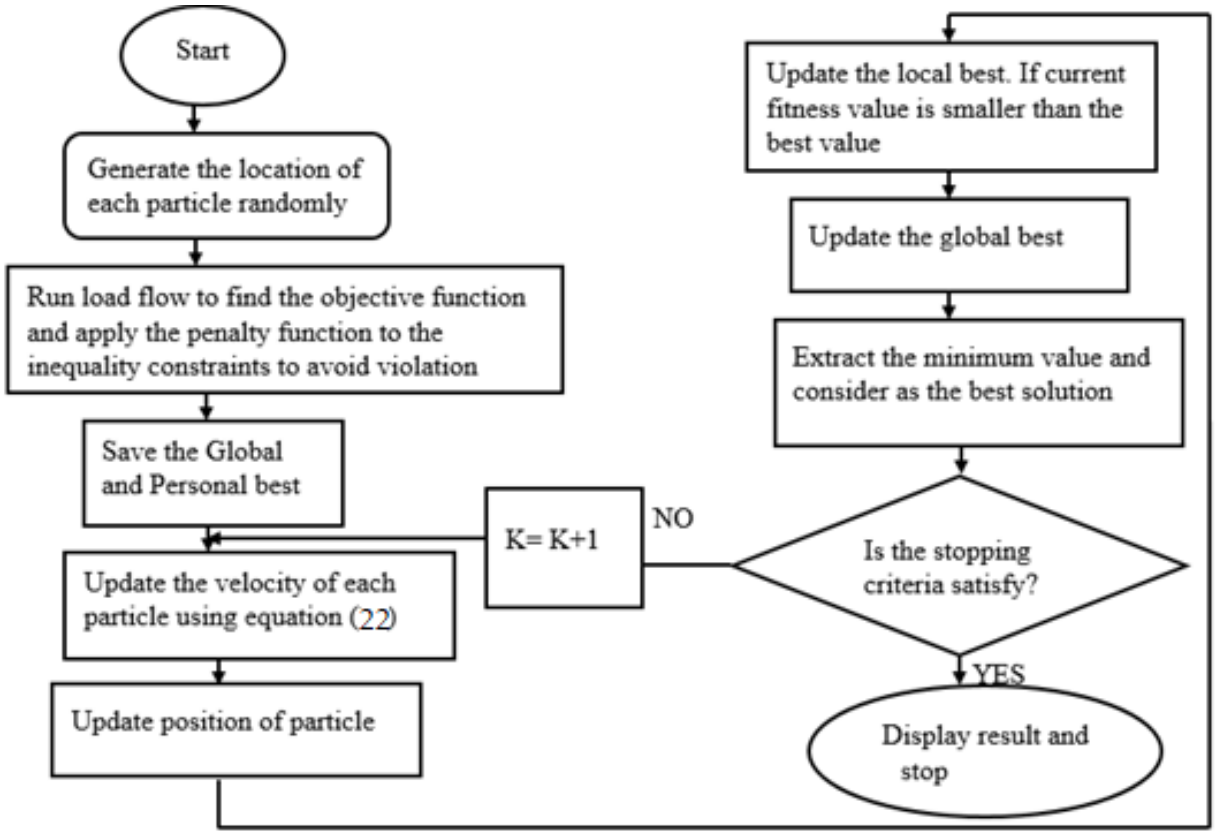

Figure 1. Flow chart of EPSO.

4. Result and Discussion

This section is divided into two. The first section discusses the results of voltage stability indices. The second section discusses the results of the RPO algorithm. The algorithm settings used in the second section is shown in Table 1. The simulation was executed using MATLAB 2018b. The IEEE 9 and 14 bus systems were employed to evaluate the effectiveness of the techniques for actual power reduction. The best outcomes are documented after each test system has been run 30 times.

Table 1. Optimum setting of the algorithm.

Parameters	Value
Number of iterations	200
Particle number	50
Acceleration constant	C1 = C2 = C3 = 2.05
Maximum and minimum w	0.9 and 0.4
Constriction factor	0.729

4.1. Voltage Stability Indices

4.1.1. IEEE 9 Bus System

The system consists of three generators located at buses 1, 2, and 3; three load buses located at buses 5, 6, and 8; and three transformers located at buses 1, 2, and 3. Also, the system has six transmission lines and 100 MVA at the base. The line and bus data are taken [41,42]. The single-line diagram/scheme of the IEEE 9 bus system was given in Figure 2. The MATLAB 2018b software was used to validate the FVSI and L_{mn} and the results obtained after varying reactive power of load buses are presented in Table 2. The critical node of the system was selected by varying/increasing the RP of the load bus until one of the indices values approaches unity, and the bus contains the lowest permissible RP. The load buses' RP was increased one after the other to find the maximum reactive power of each load bus. In Table 2, the value of the indices, the voltage magnitude, and each load bus ranking are presented. The bus with the highest values of the index and a smaller load-ability value of RP is ranked first and is the system's critical node. Node 8 is the critical node and ranks first in the system because it contains a small RP load variation of 240 MVar and a value of 1.028 for FVSI. The lines connected to it are 7–8 and 8–9. This bus needs urgent attention to avoid the breakdown of the generator.

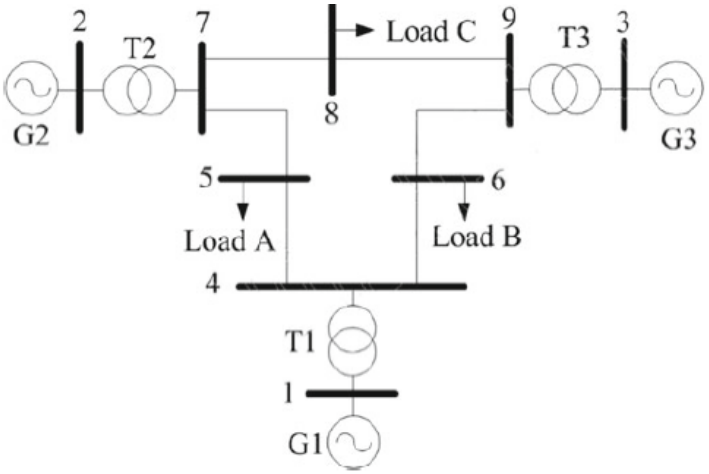

Figure 2. Single-line diagram of the IEEE 9 bus system [43].

Table 2. The indices value and ranking of the bus in the IEEE 9 bus system.

Bus Numbers	Q (MVar)	L_{mn}	FVSI	Voltage Magnitude (p.u)	Ranking
5	260	0.902	0.933	0.800	2
6	290	0.865	0.889	0.824	3
8	240	0.998	1.028	0.802	1

4.1.2. IEEE 14 Bus System

The IEEE 14 bus system contains four generators, a slack bus, twenty transmission lines, and nine load buses located at buses 4, 5, 7, 9, 10, 11, 12, 13, and 14. The line and bus data were taken [29,30]. The single-line diagram/scheme of the IEEE 14 bus system is given in Figure 3. Table 3 shows each load bus's indices value, ranking, and voltage magnitude. The validation was carried out on MATLAB 2018b software, the FVSI and L_{mn} results were obtained after varying the reactive power of load buses. The RP of the load bus was varied one bus at a time until the value of indices reached unity, or the LF solution failed to converge. When varying the RP of each load bus, one of the indices values makes the bus vulnerable to voltage collapse; at this stage, the indices values were noted, and the bus was selected as the critical bus. The result obtained was compared with the previous study reported by Samuel et al. [30], and it was observed that the result of this study shows its validity and effectiveness as it aligned with that of the literature [30]. It also presents the ranking of each bus, which was carried out based on the highest values of the indices and the least RP injected into the load bus. The load node/bus with the highest indices value and the small permissible reactive load was selected as the critical node of the system and ranked first. It clearly shows that node 14 is the critical bus/node of the system because it had the highest values of the index of 1.023 for FVSI and a small permissible reactive load of 76.5 MVar. This node/bus had two connected lines, 9–14 and 13–14. The load connected to the line experienced voltage instability. This was identified as the weakest bus that needs proper attention to avoid voltage collapse. The most stable bus are nodes/buses 4 and 5. They had the height value of RP injected into the bus, 360 MVar, and 352.5 MVar, respectively.

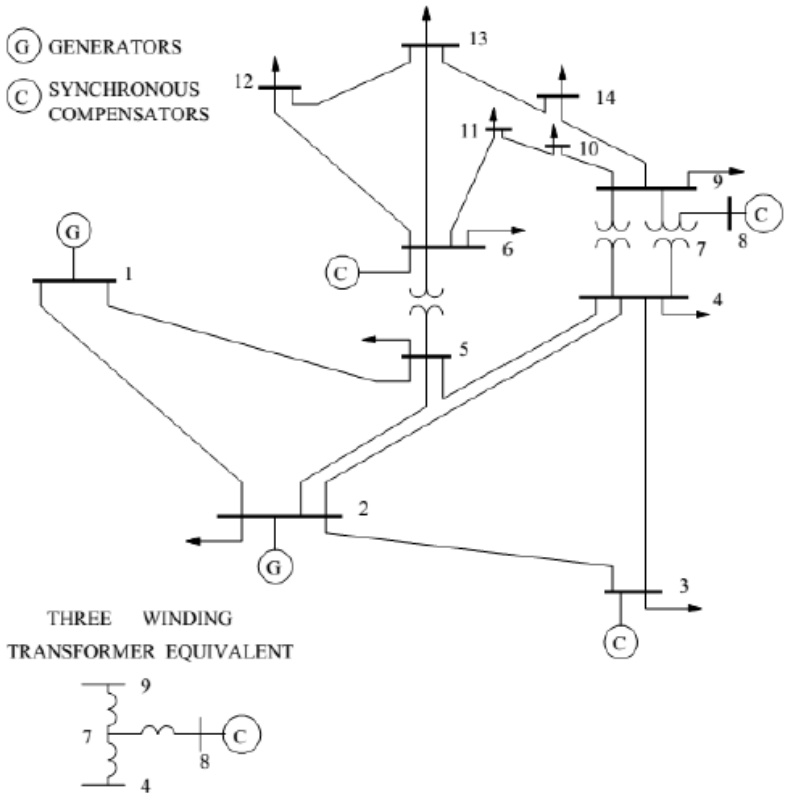

Figure 3. Single-line diagram of the IEEE 14 bus system [30].

Table 3. The indices value and ranking of the bus in the IEEE 14 bus system.

Bus Number	Q (Var)	Voltage Magnitude (p.u)	Ranking	L_{mn}	FVSI
4	360	0.833	9	0.944	0.892
5	352.5	0.997	8	0.998	0.999
7	160	0.771	7	0.929	0.928
9	150	0.712	5	0.981	0.970
10	120	0.663	4	0.942	0.904
11	103	0.748	3	0.912	0.974
12	78	0.790	2	0.865	0.868
13	151.8	0.747	6	0.923	0.993
14	76.5	0.693	1	0.966	1.023

4.2. Reactive Power Optimization

To test the chosen EPSO for RPO, EPSO and other PSO variants are coded in MATLAB 2018b software. Table 4 shows the control variable limits of the two test systems. The maximum and minimum limits for voltage magnitude are 1.1 p.u and 0.95 p.u, respectively. Also, the maximum and minimum limits for the transformer tab limits are 1.025 and 0.975, respectively. However, the limits for the shunt compensator are set in the ranges of 0 MVar and 20 MVar [44].

Table 4. Control variable limits for the IEEE 9 and 14 bus system.

Voltage	Test Systems
V_{max}	1.10
V_{min}	0.95
T_{max}	1.025
T_{min}	0.975
Q_{max}	20
Q_{min}	0.0

4.2.1. IEEE 9 Bus System

Table 4 illustrates the variable control limits of the algorithms used in this research. The N-R was used to obtain the base case power loss. EPSO and other PSO variants are compared to obtain the smallest power loss. Figure 4 illustrates the convergence curve of the system. The loss of PSO, EPSO, PSO-TVAC, PSO-SR, and RPSO are 7.608 MW, 7.543 MW, 7.589 MW, 7.600 MW, and 7.602 MW, respectively, from the base case of 9.842 MW. The optimized power loss is expected to be smaller than the base case result. Therefore, EPSO gives the smallest power loss of 7.543 MW; this shows the significance of the chosen method in power loss reduction. Figure 5 illustrates the voltage profile at each bus before and after the optimization. It can be seen that EPSO offered the highest voltage profile. This shows that EPSO is more suitable for improving the node voltage than the rest of the PSO variants. Table 5 gives the comparison of power loss for EPSO with other PSO variants and algorithms. It can be seen that EPSO gave the smallest power loss of 7.543 MW. This shows the effectiveness of EPSO in offering accurate results and outperforms all of them.

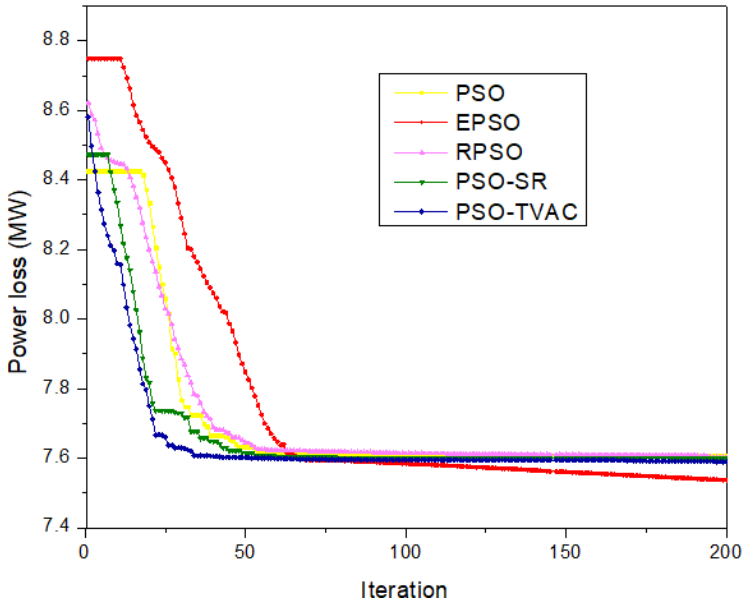

Figure 4. The convergence curve minimizes real power loss for the IEEE 9 bus system.

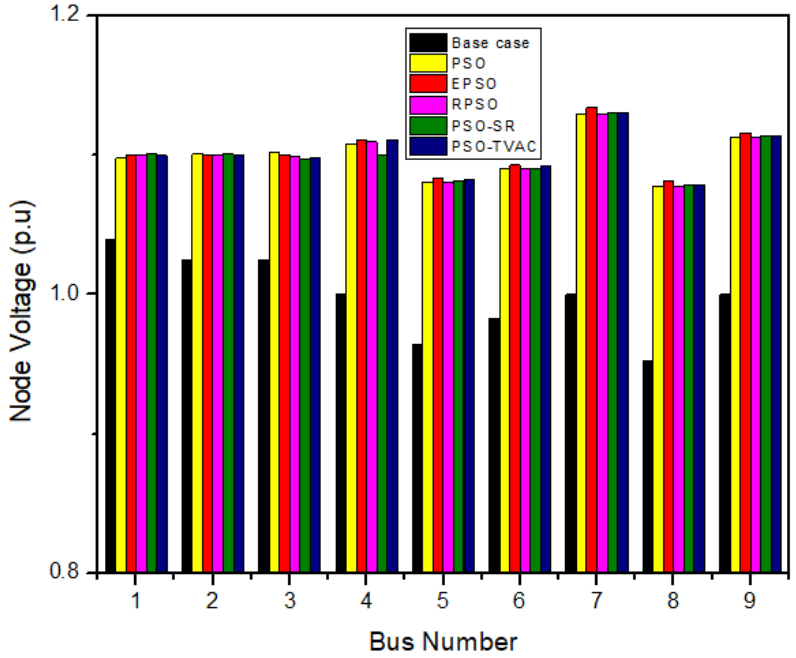

Figure 5. Voltage magnitude before optimization (base case) and after optimization of the IEEE 9 bus system.

Table 5. Comparison of the IEEE 9 bus system with other algorithms.

Algorithms	PSO	EPSO	PSO-TVAC	PSO-SR	RPSO	DA [45]	CA [45]
Best MW	7.6077	**7.543**	7.5894	7.600	7.6023	14.74	14.82
Worst MW	8.957	8.257	8.685	8.878	8.989	-	-
Mean MW	8.282	7.900	8.137	8.239	8.296	-	-
STD	0.954	0.505	0.775	0.902	0.957	-	-

The bold value indicates the lowest power loss and the superiority of this study to others presented in the table.

4.2.2. IEEE 14 Bus System

The control variable is given in Table 4. The N-R was used as the base case, while EPSO was chosen and compared with other PSO variants. The initial/base case system loads, total generation, and power losses of the test system from the LF solution by NR method are given below.

$$\boldsymbol{P_{load} = 259\ \text{MW}, P_{loss} = 13.775\ \text{MW}, \text{and}\ P_G = 272.757\ \text{MW}}$$

The curve of the real power loss of EPSO is demonstrated in Figure 6. The power loss reduction of PSO, EPSO, PSO-TVAC, PSO-SR, and RPSO are 12.263 MW, 12.253 MW, 12.260 MW, 12.261 MW, and 12.264 MW, respectively, from the base case of 13.775 MW. After optimization, the power loss is expected to be less than the base case result. It can be seen that EPSO outperforms all other PSO variants, giving a lower reduction of 12.253 MW. However, EPSO has more computation times. Furthermore, Figure 7 shows the voltage magnitude of each bus/node before and after optimization. EPSO effectively increases each node's voltage and gives the smallest loss reduction. The superiority of EPSO was validated by comparing the real power loss, mean, and standard deviation (STD) of the result obtained with other algorithms, like PSO, PSO-TVAC, RPSO, LCA, JAYA, and PBIL, as presented in Table 6. Notably, it shows that EPSO reduced the power loss to 12.253 MW, while PSO offers 12.263 MW, PSO-TVAC offers 12.260 MW, RPSO offers 12.259 MW, etc. Thus, EPSO methods give excellent results by lowering power loss and outperforming other techniques.

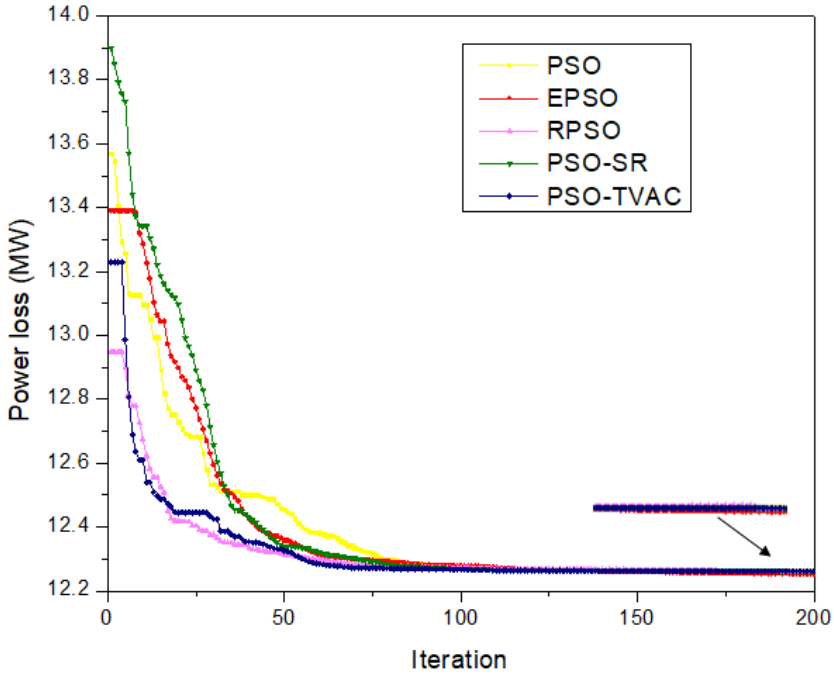

Figure 6. Convergence minimization of real power loss for the IEEE 14 bus system.

Table 6. Comparison of the IEEE 14 bus system with other algorithms.

Algorithms	Best	Worst	Mean	STD
PSO	12.263	12.879	12.571	0.436
EPSO	**12.253**	12.311	12.282	0.041

Table 6. *Cont.*

Algorithms	Best	Worst	Mean	STD
PSO-TVAC	12.260	12.587	12.424	0.232
PSO-SR	12.261	12.762	12.512	0.354
RPSO	12.259	12.324	12.292	0.046
HLGBA [28]	13.1229	-	-	-
LCA [46]	12.9891	13.1638	-	5.5283×10^{-3}
PBIL [46]	13.0008	13.1947	-	9.7075×10^{-4}
JAYA [47]	12.281	-	-	-
PSO [44]	12.36	-	-	-

The bold value indicates the lowest power loss and the superiority of this study to others presented in the table.

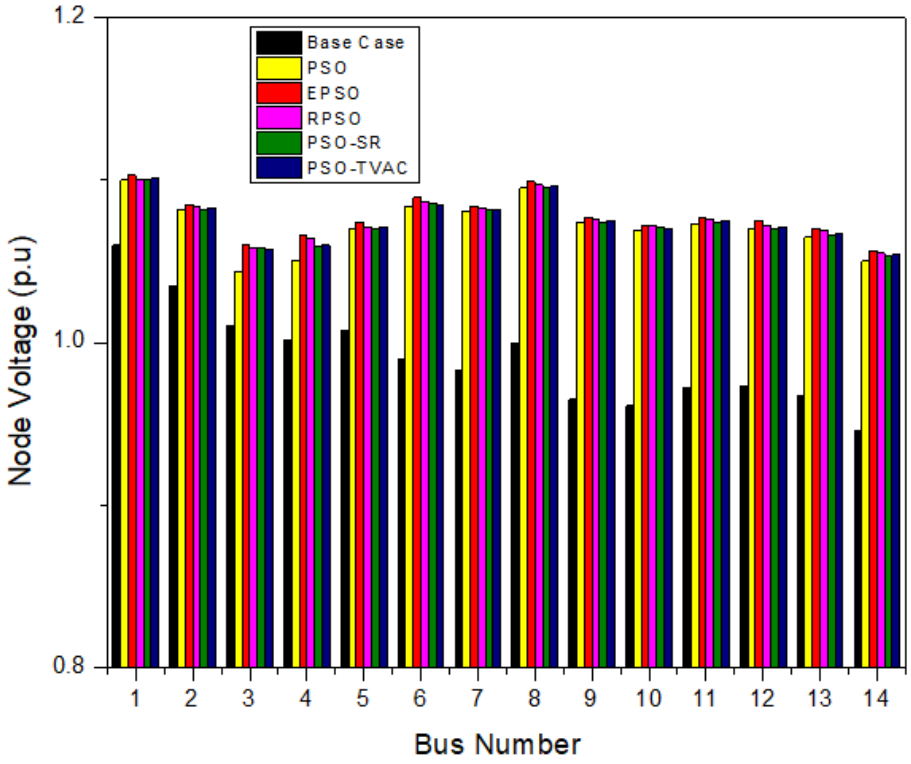

Figure 7. Voltage magnitude before optimization (base case) and after optimization for the IEEE 14 bus system.

5. Conclusions and Future Work

The role of PS operations is to ensure a stable voltage at the consumer end. Unfortunately, the PS failed to meet the desired goal due to generator failures and losses in the TL. This work applied EPSO to reduce the real power loss and other PSO variants. FVSI and L_{mn} were used to identify the critical bus and to learn the stressfulness of the lines in a PS. For the IEEE 9 bus system, bus 8 is the critical node, and the lines connected to it are the most stressful lines of the system. It has the lowest value of RP of 240 MVar, and one of the indices reaches unity (1). Node 14 was the critical node in the IEEE 14 bus system, and the lines connected to it experienced voltage instability. EPSO was used to reduce/diminish the actual/real power loss on the IEEE 9 and 14 bus systems. The loss was reduced from 9.842 MW to 7.543 MW for EPSO and 7.608 MW, 7.602 MW, 7.589 MW, and 7.600 MW for PSO, RPSO, PSO-TVAC, and PSO-SR, respectively, for the IEEE 9 bus system. Also, the losses on the IEEE 14 bus system were reduced from 13.775 MW (the base case) to 12.253 MW for

EPSO and 12.263 MW, 12.259 MW, 12.260 MW, and 12.261 MW for PSO, RPSO, PSO-TVAC, and PSO-SR, respectively. The result shows that the EPSO algorithm gives a better loss reduction than other techniques and PSO variants in the literature. This indicates that EPSO is suitable for improving grid voltage quality, thereby suggesting that the technique will be a valuable tool for PS engineers in the planning and operation of electrical PS networks. This work recommends applying EPSO to other metaheuristic algorithms to form a hybrid method to solve engineering problems and some standard IEEE benchmark functions. Also, the computation time should be improved in future work.

Author Contributions: S.A.A.: Conceptualization, data curation, formal analysis and investigation, methodology, validation, visualization, writing—original draft preparation, writing—review, and editing; Y.S. and Z.W.: Conceptualization, validation, visualization, review, editing, and supervision. All authors have read and agreed to the published version of the manuscript.

Funding: This research work was supported by Global Excellence and Stature, Fourth Industrial Revolution (GES 4.0), University of Johannesburg, South Africa.

Data Availability Statement: All data used in this study are available within this manuscript.

Conflicts of Interest: The authors declare no conflict of interest.

Nomenclature

FVSI	fast voltage stability index
L_{mn}	line stability index
TL	transmission line
RP	reactive power
Zj	is the impedance
Q_1	is the RP at sending end
Xr	is the reactance of the line
θ	is the angle of the TL
V_1	is the voltage at the sending end
δ	is the power angle
Q_2	is the RP at receiving end
P_{loss}	is the real total losses
k	is the branch
G_k	is the conductance of the branch k
Vj and V_i	are the voltage at the ith and jth bus
N_L	is the total number of TL
θ_{ij}	is the voltage angle between bus i and j
g_{ij} and b_{ij}	are conductance and susceptance
V_{gi}^{min} and V_{gi}^{max}	are voltage magnitude limits
Q_{gi}^{min} and Q_{gi}^{max}	are the generation limits of reactive power
P_{gi}^{min} and P_{gi}^{max}	are the limits of active power
Q_{ci}^{min} and Q_{ci}^{max}	are the reactive compensation limits
T_k^{min} and T_k^{max}	are the transformer tap limits
V_i^k	is the velocity of the particle
s_i^k	is the position of the particle
p_{best}	is the personal best
g_{best}	is the global best
r_1 and r_2	are two randomly generated numbers between (0, 1)
c_1 and c_2	are the coefficients of accelerated particles
w	is the inertia weight
SR	is the success rate

w^{min} and w^{max}	is the minimum and maximum limits of the w
z	is the current iteration
$iter_{max}$	is the maximum iteration
C_{1k}, C_{1t}, C_{2t}, and C_{2k}	are the initial and final values of the cognitive and social acceleration factors
$p_{best,t}$	is the vector position for an excellent individual domain (i.e., the overall best position)
φ	is the constriction factor
PSO	particle swarm optimization
PF	power flow
P.U	per unit
RPSO	random inertia weight PSO
TVAC	time-varying acceleration coefficients
VS	is the voltage stability
DER	is the distributed energy resources
PS	is the power system
RPO	is the reactive power optimization

References

1. Hosseinzadeh, N.; Aziz, A.; Mahmud, A.; Gargoom, A.; Rabbani, M. Voltage Stability of Power Systems with Renewable-Energy Inverter-Based Generators: A Review. *Electronics* **2021**, *10*, 115. [CrossRef]
2. Ibrahim, I.A.; Hossain, M.J. Low Voltage Distribution Networks Modeling and Unbalanced (Optimal) Power Flow: A Comprehensive Review. *IEEE Access* **2021**, *9*, 143026–143084. [CrossRef]
3. Shayeghi, H.; Rahnama, A.; Mohajery, R.; Bizon, N.; Mazare, A.G.; Ionescu, L.M. Multi-Area Microgrid Load-Frequency Control Using Combined Fractional and Integer Order Master–Slave Controller Considering Electric Vehicle Aggregator Effects. *Electronics* **2022**, *11*, 3440. [CrossRef]
4. González, I.; Calderón, A.J.; Folgado, F.J. IoT Real Time System for Monitoring Lithium-Ion Battery Long-Term Operation in Microgrids. *J. Energy Storage* **2022**, *51*, 104596. [CrossRef]
5. Subramani, C.; Dash, S.S.; Jagdeeshkumar, M.; Bhaskar, M.A. Stability Index Based Voltage Collapse Prediction and Contingency Analysis. *J. Electr. Eng. Technol.* **2009**, *4*, 438–442. [CrossRef]
6. Adegoke, S.A.; Sun, Y. Power System Optimization Approach to Mitigate Voltage Instability Issues: A Review. *Cogent Eng.* **2023**, *10*, 2153416. [CrossRef]
7. Zha, Z.; Wang, B.; Fan, H.; Liu, L. An Improved Reinforcement Learning for Security-Constrained Economic Dispatch of Battery Energy Storage in Microgrids. In Proceedings of the Neural Computing for Advanced Applications, Second International Conference, NCAA 2021, Guangzhou, China, 27–30 August 2021; Zhang, H., Yang, Z., Zhang, Z., Wu, Z., Hao, T., Eds.; Springer: Singapore, 2021; pp. 303–318.
8. Mu, B.; Zhang, X.; Mao, X.; Li, Z. An Optimization Method to Boost the Resilience of Power Networks with High Penetration of Renewable Energies. In Proceedings of the Neural Computing for Advanced Applications, Second International Conference, NCAA 2021, Guangzhou, China, 27–30 August 2021; Zhang, H., Yang, Z., Zhang, Z., Wu, Z., Hao, T., Eds.; Springer: Singapore, 2021; pp. 3–16.
9. Ratra, S.; Tiwari, R.; Niazi, K.R. Voltage Stability Assessment in Power Systems Using Line Voltage Stability Index. *Comput. Electr. Eng.* **2018**, *70*, 199–211. [CrossRef]
10. Pérez-Londoño, S.; Rodríguez, L.F.; Olivar, G. A Simplified Voltage Stability Index (SVSI). *Int. J. Electr. Power Energy Syst.* **2014**, *63*, 806–813. [CrossRef]
11. Kessel, P.; Glavitsch, H. Estimating the Voltage Stability of a Power System. *IEEE Trans. Power Deliv.* **1986**, *1*, 346–354. [CrossRef]
12. Sakthivel, S.; Mary, D.; Ezhilan, C. Global Voltage Stability Limit Improvement by Real and Reactive Power Optimization through Evolutionary Programming Algorithm. *Int. J. Adv. Sci. Technol. Res.* **2012**, *1*, 88–102.
13. Sajan, K.S.; Kumar, V.; Tyagi, B. Genetic Algorithm Based Support Vector Machine for On-Line Voltage Stability Monitoring. *Int. J. Electr. Power Energy Syst.* **2015**, *73*, 200–208. [CrossRef]
14. Hamid, Z.A.; Musirin, I.; Rahim, M.N.A.; Kamari, N.A.M. Application of Electricity Tracing Theory and Hybrid Ant Colony Algorithm for Ranking Bus Priority in Power System. *Int. J. Electr. Power Energy Syst.* **2012**, *43*, 1427–1434. [CrossRef]
15. Yang, D.S.; Sun, Y.H.; Zhou, B.W.; Gao, X.T.; Zhang, H.G. Critical Nodes Identification of Complex Power Systems Based on Electric Cactus Structure. *IEEE Syst. J.* **2020**, *14*, 4477–4488. [CrossRef]
16. Adebayo, I.; Jimoh, A.A.; Yusuff, A. Voltage Stability Assessment and Identification of Important Nodes in Power Transmission Network through Network Response Structural Characteristics. *IET Gener. Transm. Distrib.* **2017**, *11*, 1398–1408. [CrossRef]
17. Adegoke, S.A.; Sun, Y. Optimum Reactive Power Dispatch Solution Using Hybrid Particle Swarm Optimization and Pathfinder Algorithm. *Int. J. Comput.* **2022**, *21*, 403–410. [CrossRef]
18. Suresh, V.; Senthil Kumar, S. Research on Hybrid Modified Pathfinder Algorithm for Optimal Reactive Power Dispatch. *Bull. Polish Acad. Sci. Tech. Sci.* **2021**, *69*, 137733. [CrossRef]

19. Yapici, H. Solution of Optimal Reactive Power Dispatch Problem Using Pathfinder Algorithm. *Eng. Optim.* **2021**, *53*, 1946–1963. [CrossRef]
20. Mukherjee, A.; Mukherjee, V. Chaotic Krill Herd Algorithm for Optimal Reactive Power Dispatch Considering FACTS Devices. *Appl. Soft Comput. J.* **2016**, *44*, 163–190. [CrossRef]
21. Mouassa, S.; Bouktir, T.; Salhi, A. Ant Lion Optimizer for Solving Optimal Reactive Power Dispatch Problem in Power Systems. *Eng. Sci. Technol. Int. J.* **2017**, *20*, 885–895. [CrossRef]
22. Üney, M.Ş.; Çetinkaya, N. New Metaheuristic Algorithms for Reactive Power Optimization. *Teh. Vjesn.* **2019**, *26*, 1427–1433. [CrossRef]
23. Adegoke, S.A.; Sun, Y. Diminishing Active Power Loss and Improving Voltage Profile Using an Improved Pathfinder Algorithm Based on Inertia Weight. *Energies* **2023**, *16*, 1270. [CrossRef]
24. Harish Kiran, S.; Dash, S.S.; Subramani, C. Performance of Two Modified Optimization Techniques for Power System Voltage Stability Problems. *Alex. Eng. J.* **2016**, *55*, 2525–2530. [CrossRef]
25. Jaramillo, M.D.; Carrión, D.F.; Muñoz, J.P. A Novel Methodology for Strengthening Stability in Electrical Power Systems by Considering Fast Voltage Stability Index under N—1 Scenarios. *Energies* **2023**, *16*, 3396. [CrossRef]
26. Adebayo, I.G.; Sun, Y. Voltage Stability Based on a Novel Critical Bus Identification Index. In Proceedings of the 2019 14th IEEE Conference on Industrial Electronics and Applications (ICIEA), Xi'an, China, 19–21 June 2019; pp. 1777–1782. [CrossRef]
27. Adebayo, I.G.; Sun, Y. A Comparison of Voltage Stability Assessment Techniques in a Power System. 2018. Available online: https://core.ac.uk/download/pdf/187150311.pdf (accessed on 5 July 2023).
28. Alam, M.S.; De, M. Optimal Reactive Power Dispatch Using Hybrid Loop-Genetic Based Algorithm. In Proceedings of the 2016 National Power Systems Conference (NPSC) 2016, Bhubaneswar, India, 19–21 December 2016; pp. 1–6. [CrossRef]
29. Vishnu, M.; Sunil Kumar, T.K. An Improved Solution for Reactive Power Dispatch Problem Using Diversity-Enhanced Particle Swarm Optimization. *Energies* **2020**, *13*, 2862. [CrossRef]
30. Samuel, I.A.; Katende, J.; Awosope, C.O.A.; Awelewa, A.A. Prediction of Voltage Collapse in Electrical Power System Networks Using a New Voltage Stability Index. *Int. J. Appl. Eng. Res.* **2017**, *12*, 190–199.
31. Chaturvedi, K.T.; Pandit, M.; Srivastava, L. Particle Swarm Optimization with Time Varying Acceleration Coefficients for Non-Convex Economic Power Dispatch. *Int. J. Electr. Power Energy Syst.* **2009**, *31*, 249–257. [CrossRef]
32. Roy Ghatak, S.; Sannigrahi, S.; Acharjee, P. Comparative Performance Analysis of DG and DSTATCOM Using Improved Pso Based on Success Rate for Deregulated Environment. *IEEE Syst. J.* **2018**, *12*, 2791–2802. [CrossRef]
33. Musiri, I.; Abdul Rahman, T.K. On-Line Voltage Stability Based Contingency Ranking Using Fast Voltage Stability Index (FVSI). In Proceedings of the IEEE/PES Transmission and Distribution Conference and Exhibition, Yokohama, Japan, 6–10 October 2002; Volume 2, pp. 1118–1123. [CrossRef]
34. Moghavvemi, M.; Faruque, M.O. Power System Security and Voltage Collapse: A Line Outage Based Indicator for Prediction. *Int. J. Electr. Power Energy Syst.* **1999**, *21*, 455–461. [CrossRef]
35. Kennedy, J.; Eberhart, R. Particle Swarm Optimization. In Proceedings of the ICNN'95-International Conference on Neural Networks, Perth, WA, Australia, 27 November–1 December 1995; pp. 1942–1948. [CrossRef]
36. Poli, R.; Kennedy, J.; Blackwell, T.; Freitas, A. Particle Swarms: The Second Decade. *J. Artif. Evol. Appl.* **2008**, *2008*, 108972. [CrossRef]
37. Vinodh Kumar, E.; Raaja, G.S.; Jerome, J. Adaptive PSO for Optimal LQR Tracking Control of 2 DoF Laboratory Helicopter. *Appl. Soft Comput. J.* **2016**, *41*, 77–90. [CrossRef]
38. Neyestani, M.; Farsangi, M.M.; Nezamabadipour, H.; Lee, K.Y. A Modified Particle Swarm Optimization for Economic Dispatch with Nonsmooth Cost Functions. *IFAC Proc. Vol.* **2009**, *42*, 267–272. [CrossRef]
39. Ratnaweera, A.; Halgamuge, S.K.; Watson, H.C. Self-Organizing Hierarchical Particle Swarm Optimizer with Time-Varying Acceleration Coefficients. *IEEE Trans. Evol. Comput.* **2004**, *8*, 240–255. [CrossRef]
40. Cao, S.; Ding, X.; Wang, Q.; Chen, B. Opposition-Based Improved Pso for Optimal Reactive Power Dispatch and Voltage Control. *Math. Probl. Eng.* **2015**, *2015*, 754582. [CrossRef]
41. Asija, D.; Choudekar, P.; Soni, K.M.; Sinha, S.K. Power Flow Study and Contingency Status of WSCC 9 Bus Test System Using MATLAB. In Proceedings of the 2015 International Conference on Recent Developments in Control, Automation and Power Engineering (RDCAPE), Noida, India, 12–13 March 2015; pp. 338–342.
42. Parmar, R.; Tandon, A.; Nawaz, S. Comparison of Different Techniques to Identify the Best Location of SVC to Enhance the Voltage Profile. *ICIC Express Lett.* **2020**, *14*, 81–87. [CrossRef]
43. Sriram, C.; Kishore, M.N.R. Teaching Distance Relay Protection and Circuit Breaker Co-Ordination of an IEEE 9 Bus System Using MATLAB/SIMULINK. In Proceedings of the Innovations in Electrical and Electronics Engineering: Proceedings of the 4th ICIEEE 2019, Telangana, India, 26–27 July 2019; Saini, H.S., Srinivas, T., Vinod Kumar, D.M., Chandragupta Mauryan, K.S., Eds.; Springer: Singapore, 2020; pp. 439–447.
44. Modha, H.; Patel, V. Minimization of Active Power Loss for Optimum Reactive Power Dispatch Using PSO. In Proceedings of the 2021 Emerging Trends in Industry 4.0 (ETI 4.0), Raigarh, India, 19–21 May 2021; pp. 1–5. [CrossRef]
45. Khan, I.; Li, Z.; Xu, Y.; Gu, W. Distributed Control Algorithm for Optimal Reactive Power Control in Power Grids. *Int. J. Electr. Power Energy Syst.* **2016**, *83*, 505–513. [CrossRef]

46. Suresh, V.; Kumar, S.S. Optimal Reactive Power Dispatch for Minimization of Real Power Loss Using SBDE and DE-Strategy Algorithm. *J. Ambient Intell. Humaniz. Comput.* **2020**, 1–15. [CrossRef]
47. Barakat, A.F.; El-Sehiemy, R.A.; Elsayd, M.I.; Osman, E. Solving Reactive Power Dispatch Problem by Using JAYA Optimization Algorithm. *Int. J. Eng. Res. Afr.* **2018**, *36*, 12–24. [CrossRef]